A-094

J. Chem. Thermodynamics **1979**, 11, 367–378

Low-temperature phase transitions of Fe_3O_4 with innocuous dopants[a]

BENGT G. FALK,[b] LU-SAN PAN, B. J. EVANS, and EDGAR F. WESTRUM, Jr.

Department of Chemistry, University of Michigan, Ann Arbor, Michigan 48109 U.S.A.

(*Received 31 March 1978; in revised form 3 July 1978*)

Both Zn^{2+} and Cd^{2+} dopants on the A-sites in Fe_3O_4 lead to a loss in the furcation of the lambda anomaly at the Verwey transition but at markedly different dopant levels. Equilibrium adiabatic calorimetry from 5 to 350 K on new compositions of cadmium- and zinc-doped magnetites, *e.g.* $Cd_{0.002}Fe_{2.998}O_4$ and $Zn_{0.01}Fe_{2.99}O_4$, permits an estimate of the mole ratios of Cd and Zn at which they have equivalent effects on the furcation of the lambda anomaly. These results are consistent with a mechanism in which the furcation of the Verwey transition in doped samples depends linearly on the deviation of the lattice constant from that of pure Fe_3O_4. Further studies on a deliberately oxidized sample demonstrate that the furcated lambda anomaly is characteristic of stoichiometric materials; apparently B-site vacancies have a much greater effect on the transition than A-site dopants. Heat capacities and thermodynamic properties of the three samples are summarized.

1. Introduction

Previous investigations have shown the characteristics of the low-temperature transition in Fe_3O_4 to be very sensitive to the presence of small mole ratios of impurity ions.[1–5] This is so even when the impurity ions are diamagnetic and occupy the A-sites—which are not actively involved in the electron-ordering. In pure Fe_3O_4[6] the heat-capacity anomaly at the low-temperature phase transition is bifurcated. Upon the addition of small amounts of innocuous impurity ions—*i.e.* diamagnetic A-site occupants such as Zn^{2+} and Cd^{2+}—the furcation is observed to vanish. The temperatures of the peaks in the lambda anomaly and enthalpies of transition depend sensitively on the mole ratio and kind of dopant ion, but all of the variations in the characteristics of the transition appear to be interpretable in terms of an increase in the lattice constant and perhaps a decrease in the concentration of the itinerant electrons.

In the present study, samples of $Cd_{0.002}Fe_{2.998}O_4$ and $Zn_{0.010}Fe_{2.99}O_4$ were investigated by adiabatic-jacket calorimetry to determine the critical mole ratios of Cd and Zn for the disappearance of the furcation. Previous measurements of zinc- and cadmium-doped samples have shown that the furcation of the heat-capacity anomaly vanishes between 0.005 and 0.066 Zn per Fe_3O_4, whereas even for the

[a] Support for this project has been provided by the National Science Foundation.

[b] Current address: Pharmacia Fine Chemicals, Box 175, S-751 25 Uppsala, Sweden.

0021-9614/79/040367+12 $01.00/0.

lowest dopant level of 0.005 for cadmium, the furcation was already absent. Thus, in the present investigation we have sought to determine the lowest cadmium dopant level at which the furcation is still retained and the mole ratio of Zn between 0.066 and 0.005 at which the furcation just vanishes.

In addition, the $Cd_{0.002}Fe_{2.998}O_4$ sample was oxidized to a small extent in a pure CO_2 atmosphere at 1623 K in order to determine the effects of vacancies at B-sites in mole ratios comparable to those of the Cd and Zn dopants, *i.e.* about 0.03 per Fe_3O_4.

2. Experimental

CALORIMETRIC TECHNIQUE

Heat-capacity measurements were made in the Mark-II adiabatic cryostat over the range 5 to 350 K. Details of cryostat construction and measuring-circuit calibration have been described.[7] (Samples were loaded into the gold-plated copper calorimeter W-30 which has an internal volume of 18.9 cm^3 and an axial entrant well for the thermometer+heater assembly.) After evacuation the calorimeter was filled each time with a small pressure of purified helium gas to enhance thermal contact and equilibration between calorimeter, sample, and the heater+thermometer assembly. Temperatures were measured with a capsule-type platinum resistance thermometer (A-3) calibrated by the National Bureau of Standards. Calibration is referred to the "IPTS-48, text revision of 1960"[8] defined between 90.18 and 903.65 K. The National Bureau of Standards 1955 provisional scale was employed at lower temperatures. Relevant calorimeter and sample information and molar masses used for the calculation of heat capacities from observed values are given in table 1 for the several samples.

TABLE 1. Sample analysis and loading information

Property	Sample Cd(0.002-I)	Sample Zn(0.10)	Sample Cd(0.002-II)
Sample mass, m/g	33.909	35.508	25.149
Molar mass, M/g mol^{-1} [a]	231.66	231.63	231.30
Formula	$Cd_{0.002}Fe_{2.998}O_4$	$Zn_{0.10}Fe_{2.990}O_4$	$Fe_{2.9988}\square_{0.012}O_4$
p(He)/kPa [b]	16.0	16.5	14.9
Mass per cent dopant (Cd or Zn)			
—by synthesis [c]	0.097	0.28	(0.097)
—by chemical analysis	0.096	0.27	0.00
Mass per cent Fe			
—by synthesis [c]	72.28	72.09	(72.28)
—by chemical analysis	72.46	72.18	72.42
Lattice parameters:			
a_0/nm	0.83969	0.83958	0.83983
Annealing temperature, T/K	1370	1370	1623

[a] Accurate to two decimal digits, 1972 IUPAC Commission on Atomic Weights.

[b] p(He) is the pressure of helium added to improve thermal contact and equilibration between sample and calorimeter.

[c] Equivalent to theoretical or stoichiometric basis.

After establishing the temperature of transition within 1 K, transition regions were determined in detail by one or more series of determinations with increments of between 0.1 and 0.2 K. Carefully selected temperatures enabled determination of the temperature of the transitional heat-capacity maxima to within ± 0.01 K. Individual enthalpy determinations were bracketed by short energy inputs. End-point adjustment were made to the enthalpy determinations for uniformity. The measured heat capacities were corrected for the heat capacity of the empty calorimeter, which was determined in a separate series of experiments. Slight adjustments were also made for differences in the amount of gaseous helium used with the calorimeter when it was run empty and when it was run with various Fe_3O_4 samples.

SAMPLE PROVENANCE AND CHARACTERIZATION

Quantities of Johnson-Matthey Grade I "Specpure" (99.998 moles per cent pure with respect to both cations and anions) Fe_2O_3, Fe, and dopant oxide MO, consistent with the equation:

$$x\mathrm{MO} + \tfrac{1}{3}(1-x)\mathrm{Fe} + \tfrac{1}{3}(4-x)\mathrm{Fe_2O_3} = \mathrm{M}_x\mathrm{Fe}_{(3-x)}\mathrm{O_4}, \quad (1)$$

were dry-mixed in an agate mortar and loaded into a vitreous-silica ampoule which was then evacuated to 10^{-6} kPa and sealed off. The free volume in the silica ampoules was kept to a minimum by means of fillers of pure vitreous silica rods. The ampoule and contents were fired at 1370 K for 8 to 24 h. After grinding and sieving (to 75 μm or less), the sample was compressed in a carbide die; and the resulting pellet was loaded in a silica ampoule as described above. The sample was fired at 1370 K for 24 h and quenched, and the surface layers were removed. This sample is designated as Cd(0.002-I). Sample Zn(0.010) was fired similarly at 1370 K.

Sample Cd(0.002-II) resulted from Cd(0.002-I) after refiring in 100 kPa of CO_2 at 1623 K. For the binary Fe+O system, firing in pure CO_2 at 1593 to 1665 K leads to a magnetite phase with an average $n(Fe^{2+}+Fe^{3+})/n(Fe^{2+})$ of 3.01.[9] Thus, the Cd(0.002-II) sample is very slightly oxidized and can be described as a solid solution of $0.9963Fe_3O_4$ and 0.003γ–Fe_2O_3 (*i.e.* $Fe_{2.9988}\square_{0.0012}O_4$), assuming the very small amount of cadmium has no effect on the equilibrium $n(Fe^{2+}+Fe^{3+})/n(Fe^{2+})$ ratios. Attempts to analyze for Cd by wet chemical methods consistently showed none to be present within detection limits of 16×10^{-6}

Crystallographic analyses of all samples were made with a powder diffractometer using Fe $K\alpha_1$ radiation and an Mn filter. The diffraction patterns were obtained with a strip chart recorder and the lattice parameters deduced from high-angle lines exhibiting resolution of the α_1 and α_2 peaks. The lattice parameters are listed in table 1.

An accurate knowledge of the chemical composition of the phases is essential to the goals of this study. Therefore wet chemical analysis and ^{57}Fe Mössbauer spectra table 2) have been obtained. The ^{57}Fe Mössbauer spectra are very sensitive to the $n(Fe^{3+})/n(Fe^{2+})$ ratio [10] and the relative integrated intensities of the A and B site patterns are accurate indicators of $n(Fe^{3+})/n(Fe^{2+})$. In earlier studies from this group [1, 3–5] $n(Fe^{3+})/n(Fe^{2+})$ was determined by wet chemical analyses but recent determinations have proved unreliable.

TABLE 2. Magnetic hyperfine fields H_{eff}; quadrupole interactions Q; isomer shift difference δ_B, δ_A; and the ratio of the integrated intensities for the B and A sites for the magnetic samples investigated. $A(B)/A(A)$ represents the area ratios measured from Mössbauer data

Specimen	$H_{eff}(A)$ / MA m^{-1}	$H_{eff}(B)$ / MA m^{-1}	$Q(A)$ / mm s^{-1}	$Q(B)$ / mm s^{-1}	$\delta_B - \delta_A$ / mm s^{-1}	$A(B)/A(A)$
Pure Magnetite	39.20	36.53	—0.00002	0.01217	0.408	1.84 ± 0.04
$Zn_{0.01}Fe_{2.99}O_4$ Zn(0.010-I)	39.11	36.55	—0.00002	0.01135	0.426	1.99 ± 0.04
$Zn_{0.01}Fe_{2.990}O_4$ Zn(0.010-II)	39.06	36.53	—0.00000	0.01497	0.433	1.94 + 0.04
$Cd_{0.002}Fe_{2.998}O_4$ Cd(0.002-I)	39.12	36.53	+0.00000	0.00995	0.414	2.02 ± 0.04
$Cd_{0.002}Fe_{2.998}O_4$ Cd(0.002-II)	39.03	36.53	—0.00003	0.00372	0.415	1.98 ± 0.04

The area ratios in table 2 are in good agreement with those expected for stoichiometric magnetites. It is also noteworthy that sample Cd(0.002-II) shows a slight decrease in the B/A area ratio in keeping with the introduction of B site vacancies as a result of the slight oxidation. The line widths and other hyperfine interaction parameters for Zn(0.010) and Cd (0.002-I) are also those expected for stoichiometric $[n(Fe^{3+})/n(Fe^{2+}) = 1]$ magnetites. Larger B-site linewidths for C(0.002-II) provide confirmation of the slight oxidation of this sample.

These results permit an unambiguous consideration of the variations of the thermophysical values in terms of the sample compositions.

3. Results

HEAT CAPACITIES

Values for the individual determinations of heat capacity are presented in table 3 in chronological order so that the temperature increments used for the individual determinations within the series may be estimated from adjacent mean temperatures. An analytically determined curvature correction has been applied to the measured values of $\Delta H/\Delta T$ in the non-transitional regions. These results are characterized by a standard deviation of approximately 5 per cent near 10 K, decreasing to 0.8 per cent at 20 K, and to less than 0.1 per cent above 30 K.

TRANSITIONS

The determinations of the ΔH_t's and ΔS_t's are presented in table 4. Portions of the experimentally determined heat capacities for both samples have been presented as a function of temperature in figures 1 and 2. As shown in figure 1, it has indeed been possible to synthesize cadmium-doped magnetite that exhibits a bifurcated heat-capacity anomaly. It is noteworthy that this sample was prepared in a manner nearly identical to that used previously for the pure magnetites and other doped magnetites listed in table 5. The ΔH_t's of the two peaks are very similar to each other and qualitatively have an appearance almost identical to that of the Zn(0.005)-doped sample listed in table 5. However, the transition temperatures for the Cd(0.002-I) sample are much lower than those for the Zn(0.005) sample. This result is in keeping

with previous conclusions concerning the effect of cadmium on the transition. The heat capacity for the Zn(0.010)-doped magnetite is shown in figure 2. It is noteworthy that the heat-capacity anomaly of this sample is not simple and exhibits an *incipient* furcation of the peak.

TABLE 3. Experimental heat capacity of doped Fe_3O_4 crystal. ($cal_{th} = 4.184$ J)

T/K	C_p/$cal_{th}\,K^{-1}\,mol^{-1}$	T/K	C_p/$cal_{th}\,K^{-1}\,mol^{-1}$	T/K	C_p/$cal_{th}\,K^{-1}\,mol^{-1}$	T/K	C_p/$cal_{th}\,K^{-1}\,mol^{-1}$
Cd(0.002-I) [a] annealed at 1370 K							
Series I		101.77	30.74	103.07	26.32	33.89	1.378
62.48	5.818	102.79	26.95	103.68	24.65	39.37	2.059
67.77	6.809	103.91	24.50	104.04	24.36	43.38	2.617
73.18	7.831	105.01	26.97	104.39	25.02	48.09	3.340
79.68	9.178	106.01	32.64	104.74	26.08	53.72	4.266
87.35	10.895	107.16	18.60	105.08	27.37	59.02	5.184
93.27	12.350	108.58	15.75	105.40	28.86	64.68	6.227
99.99	18.99	110.06	15.91	105.71	31.07	71.12	7.427
108.44	20.54	111.53	16.13	106.01	34.33	78.91	9.015
117.00	17.04	113.69	16.48	106.29	33.99	88.92	11.270
125.68	18.41	115.83	16.82	106.59	28.04	ΔH detn. C.	
133.89	19.67	117.23	17.05	106.97	18.14		
141.71	20.84	118.61	17.27	107.42	15.88	Series VII	
149.34	21.88	119.99	17.50	107.88	15.82	99.31	14.945
157.86	23.00	122.35	17.88	108.35	15.81	99.82	15.53
167.77	24.33			108.81	15.87	100.19	16.10
177.83	25.56	Series III		109.27	15.92	100.60	17.26
187.55	26.69	89.23	11.346			101.00	20.98
197.22	27.79	ΔH detn. A		Series V		101.36	27.12
206.89	28.75	114.88	16.71	89.60	11.429	101.67	31.46
216.60	29.73			ΔH detn. B		101.96	32.94
226.37	30.64	Series IV		120.12	17.53	102.25	30.54
234.60	31.38	91.99	12.027			102.56	28.04
242.61	32.12	95.51	12.980	Series VI		102.88	26.90
253.07	32.94	96.04	13.195	5.04	0.008	103.22	25.84
263.93	33.82	96.56	13.407	6.45	0.015	103.56	24.90
274.59	34.65	97.07	13.608	7.51	0.024	103.90	24.36
285.07	35.40	97.53	20.14	8.50	0.031	104.25	24.65
295.38	36.12	97.98	14.038	9.57	0.043	104.60	25.63
305.52	36.82	98.47	14.344	10.66	0.052	104.93	26.68
315.56	37.44	98.96	14.664	11.94	0.057	105.25	28.06
325.48	38.03	99.44	15.05	13.22	0.069	105.56	30.01
335.29	38.59	99.92	15.65	14.44	0.093	105.86	32.44
345.00	39.17	100.38	16.48	15.81	0.121	106.13	35.21
		100.81	18.56	17.45	0.162	106.41	31.83
Series II		101.20	24.38	19.08	0.221	106.73	24.55
89.86	11.506	101.53	29.85	20.76	0.290	107.13	16.23
94.43	12.719	101.83	32.72	22.71	0.394	107.57	15.86
97.46	13.729	102.12	31.92	24.81	0.527	108.03	15.83
99.08	14.724	102.42	29.09	27.15	0.705	108.91	15.85
100.58	18.27	102.74	27.31	29.50	0.909	110.23	16.00

TABLE 3—*continued*

T/K	C_p/cal$_{th}$ K^{-1} mol^{-1}	T/K	C_p/cal$_{th}$ K^{-1} mol^{-1}	T/K	C_p/cal$_{th}$ K^{-1} mol^{-1}	T/K	C_p/cal$_{th}$ K^{-1} mol^{-1}
Zn(0.010) [b] annealed at 1370 K							
Series I		304.66	36.81	107.36	54.54	Series VI	
92.49	12.043	315.14	37.55	107.67	27.76	5.42	0.005
97.80	13.114	325.80	38.11	108.13	18.95	6.24	0.007
102.52	17.08	335.70	38.67	108.66	16.20	7.26	0.011
105.93	37.73	345.13	39.10	109.22	15.77	8.30	0.015
107.53	59.50			109.78	15.77	9.27	0.022
108.72	17.39	Series II		110.60	15.96	10.24	0.035
110.45	16.06	89.07	11.312			11.72	0.045
113.49	16.53	93.84	12.332	Series III		13.16	0.058
117.72	17.24	96.90	13.038	85.18	10.49	14.34	0.082
123.31	18.16	98.93	13.404	Enthalpy detn. A		15.65	0.114
132.24	19.54	99.91	13.735	125.87	18.57	17.08	0.152
142.77	21.08	100.80	14.159			20.37	0.271
152.73	22.45	101.67	14.973			22.29	0.369
162.26	23.66	102.38	16.52	Series IV		24.48	0.501
172.41	24.92	102.93	17.98	85.89	10.64	26.77	0.667
183.18	26.18	103.45	19.37	Enthalpy detn. B		29.27	0.881
193.57	27.33	103.94	20.59	124.30	18.31	32.213	1.228
203.66	28.40	104.42	21.57			35.44	1.560
213.47	29.36	104.88	23.05	Series V		38.66	1.992
223.77	30.39	105.32	25.00	55.45	4.973 [c]	41.38	2.428
234.54	31.33	105.75	24.97	60.03	5.765 [c]	43.23	2.573 [c]
245.07	32.34	106.13	35.11	65.23	6.662	46.33	3.055 [c]
255.37	33.13	106.44	40.53	72.10	7.885	51.39	4.312 [c]
265.50	33.94	106.71	53.37	79.19	9.251	56.90	5.209 [c]
275.45	34.67	106.92	79.06	86.01	10.66	Enthalpy detn. D	
285.24	35.40	107.06	121.21	Enthalpy detn. C			
294.89	36.08	107.18	114.00	123.36	18.17		
Cd(0.002-II) [d] annealed at 1623 K							
Series I		110.49	18.535	89.75	11.34	327.00	38.14
91.87	11.816	111.59	19.677	96.40	12.773	336.42	38.72
95.86	12.631	112.65	21.25	ΔH detn. A		345.27	39.18
99.67	13.461	113.68	22.23	136.52	20.11		
102.59	14.166	114.68	23.09	145.97	21.43	Series IV	
104.21	14.596	115.65	24.04	155.76	22.75	95.27	12.546
105.31	14.975	116.60	25.17	165.92	24.06	ΔH detn. B	
106.39	15.437	117.52	26.67	166.36	24.11	133.22	19.636
107.44	15.996	118.40	28.10	177.68	25.49	113.40	21.98
108.47	16.665	119.23	32.83	188.60	26.73	116.09	24.70
109.48	17.410	119.99	37.23	199.19	27.88	117.78	27.22
110.93	19.065	120.68	42.14	209.48	28.92	118.32	27.98
112.77	21.32	121.32	46.89	219.52	29.94	118.61	29.00
114.66	23.07	122.17	18.997	229.34	30.84	118.89	31.55
116.61	25.23	123.25	18.766	238.96	31.78	119.15	33.41
118.43	28.73	124.92	18.747	248.39	32.57	119.19	23.78
120.66	37.58	127.15	18.890	257.68	33.27	119.48	33.70
124.08	18.758			266.81	34.04	119.73	35.79
128.15	18.974	Series III		275.82	34.75	119.98	36.67
		61.82	6.02	285.92	35.47	120.21	39.35
Series II		67.98	7.13	296.70	36.29	120.44	39.75
103.24	14.405	75.16	8.48	306.91	36.89	120.67	40.31
107.75	16.346	82.75	9.94	317.02	37.54	120.89	45.34

TABLE 3—*continued*

T/K	C_p/cal_{th} K^{-1} mol^{-1}	T/K	C_p/cal_{th} K^{-1} mol^{-1}	T/K	C_p/cal_{th} K^{-1} mol^{-1}	T/K	C_p/cal_{th} K^{-1} mol^{-1}
121.08	58.61	118.44	28.50	122.69	18.865	18.720	0.1997
121.25	64.42	118.73	29.92			20.893	0.2903
121.48	26.59	119.01	32.56			23.312	0.4201
121.81	19.202	119.27	34.07	Series V		25.952	0.6005
122.17	18.980	119.53	35.09	4.39	0.022	28.461	0.7989
111.64	20.039	119.78	35.54	5.95	0.0131	29.453	0.8913
113.70	22.31	120.02	37.30	8.11	0.0342	33.195	1.2737
115.02	23.38	120.27	39.56	8.719	0.0374	36.831	1.7050
115.65	24.05	120.50	40.08	9.797	0.0238	42.017	2.311
116.31	24.86	120.74	41.14	10.999	0.0360	48.463	3.306
116.81	25.49	120.95	48.24	12.208	0.0459	55.804	4.998
117.14	26.16	121.14	63.02	13.316	0.0593	63.265	6.275
117.49	26.87	121.31	55.07	14.355	0.0818	98.045	13.125
117.83	27.42	121.58	20.74	15.645	0.1227	ΔH detn. C	
118.15	27.77	121.94	19.031	17.053	0.1494	133.827	19.722

[a] $Cd_{0.002}Fe_{2.998}O_4$
[b] $Zn_{0.10}Fe_{2.990}O_4$
[d] $Fe_{2.9988}\square_{0.0012}O_4$
[e] Slow thermal equilibration.

TABLE 4. Thermodynamics of the transitions
(cal_{th} = 4.184 J)

Property		H/cal_{th} mol^{-1}
	Zn(0.010) Sample	
Mean: 3 independent ΔH detns.	(A, B, and C)	
	$\{H°(122\ K) - H°(89\ K)\}$	587.3 ± 0.2
Integration C_p curve:	$\{H°(122\ K) - H°(89\ K)\}$	588.5 ± 1
Combined:	$\{H°(150\ K) - H°(100\ K)\}$	1014.5
Lattice:	$\{H°(150\ K) - H°(100\ K)\}$	892.5 ± 2
	$\Delta H_t°$	122 ± 2
$C_{p,t}$(max.)/cal_{th} K^{-1} mol^{-1}	= 140 ± 5	
$\Delta S_t°$/cal_{th} K^{-1} mol^{-1}	= 1.18 ± 4	
	Cd(0.002–I) Sample	
Mean: 3 independent ΔH detns.	(A, B, and C)	
	$\{H°(130\ K) - H°(100\ K)\}$	618.2 ± 0.2
Integration C_p curve:	$\{H°(130\ K) - H°(100\ K)\}$	618.6 ± 0.8
Combined:	$\{H°(150\ K) - H°(100\ K)\}$	1029 ± 0.4
Lattice:	$\{H°(150\ K) - H°(100K)\}$	890.0 ± 2
	$\Delta H_t°$	139 ± 2
$C_{p,t}$(max.)/cal_{th} K^{-1} mol^{-1}	= 73 ± 5	
$\Delta S_t°$/cal_{th} K^{-1} mol^{-1}	= 1.14 ± 6	
	Cd(0.002–II) Sample	
Mean: 3 independent ΔH detns.	(A, B, and C)	
	$\{H°(130\ K) - H°(90\ K)\}$	623.5 ± 0.3
Integration C_p curve: (2 detns.)	$\{H°(130\ K) - H°(90\ K)\}$	623.1 ± 1
Lattice:	$\{H°(130\ K) - H°(100\ K)\}$	148 ± 1
	$\Delta H_t°$	148 ± 2
$C_{p,t}$(max.)/cal_{th} K^{-1} mol^{-1}	= 150 ± 10	
$\Delta S_t°$(max.)/cal_{th} K^{-1} mol^{-1}	= 129 ± 0.02	

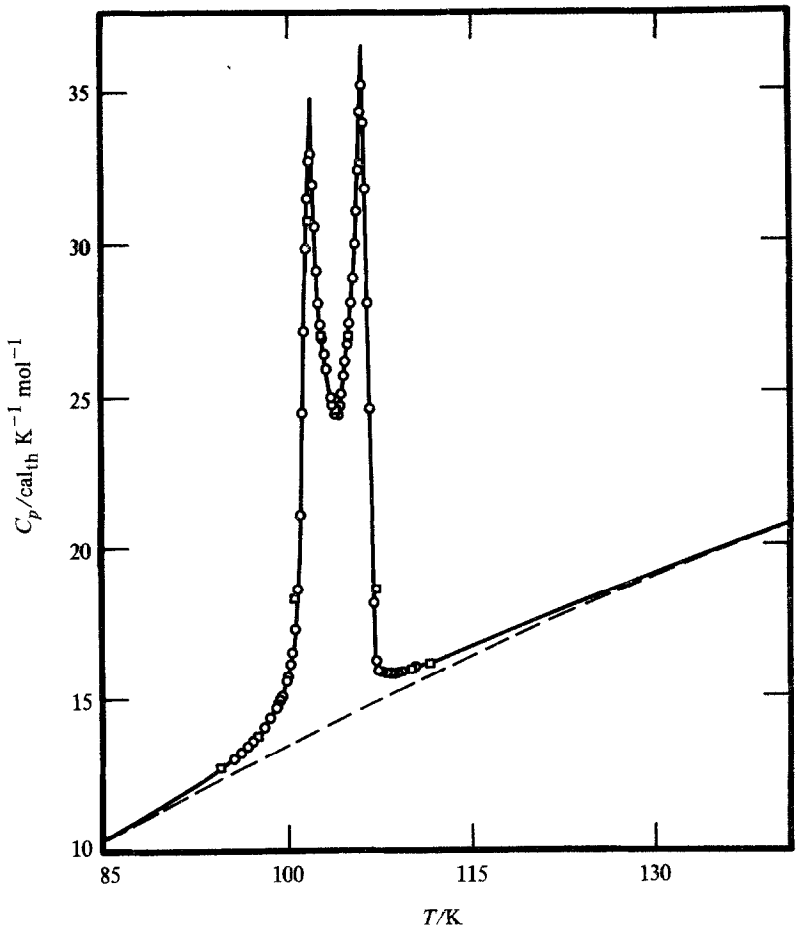

FIGURE 1. The bifurcated anomaly in the Cd (0.002–I) sample. The dashed line is the interpolated lattice heat capacity.

Insight into the influence of vacancies on the lambda anomaly can be obtained from Cd(0.002-II). This sample differs significantly from earlier oxidized samples[11] with respect to its low mole fraction of vacancies, *i.e.* about 0.06 per cent of the B-sites, and with respect to its being derived from a sample for which detailed thermodynamic data on the phase transition prior to oxidation exist. To our knowledge, detailed thermodynamic and crystal-chemical data have not been obtained prior to this work for both a very slightly oxidized magnetite and its stoichiometric precursor material. The loss in the furcation of the peak is obvious.

THERMODYNAMIC PROPERTIES

Fitting the heat-capacity values below 12 K and extrapolation below 5 K was made by the expression $C_p = aT^{3/2} + bT^3$ suggested by Kouvel [12] and found to be con-

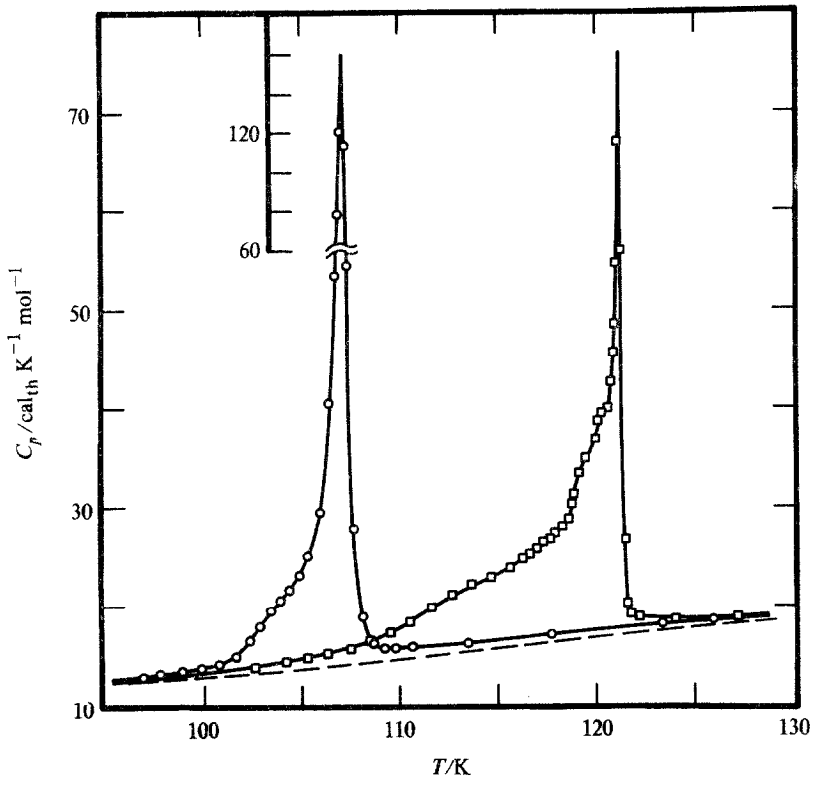

FIGURE 2. Heat capacities against temperature for two doped Fe_3O_4 samples: ○, Zn(0.010); □, Cd(0.002-II); — — —, interpolated lattice heat capacity.

sistent with our results. The thermodynamic functions are characterized by a standard deviation of ±0.08 per cent above 90 K. The thermodynamic properties of the three samples are compared with those of pure Fe_3O_4 in table 6. In general, the total thermal properties are conserved.

4. Discussion

As shown in table 5, the thermodynamic properties of the low-temperature transitions in Fe_3O_4 are very sensitive to the presence of even small amounts of impurity ions. Significant among these results are the following. First, even for ions that are not expected to influence the transition directly, a substantial effect on the thermophysical properties is observed. Secondly, not only are there quantitative changes in the thermal properties of the transition but there are also qualitative changes. The most significant of these is the defurcation of the heat-capacity anomaly observed in pure Fe_3O_4 as impurity ions such as Zn^{2+} and Cd^{2+} are added. While there are many features in the results in table 2 that can be discussed, in this paper we restrict our attention to the dependence on dopant mole fraction of the defurcation of the heat-capacity anomaly. It is observed that cadmium has a much greater influence

than zinc on the occurrence of the furcation of the heat-capacity anomaly. For example, the Zn(0.005) sample still retains the furcation of the heat-capacity anomaly. On the other hand, the furcation is entirely absent in the Cd(0.005) sample. With zinc dopant, the defurcation in the heat-capacity anomaly vanishes between Zn(0.005) and Zn(0.066). From the results of the present investigation, the Zn mole

TABLE 5. Selected thermal parameters of Fe_3O_4 transitions [a]

Material Designation	T_l/K	T_h/K	ΔH / cal_{th} mol^{-1} t	l	h	ΔS_t / cal_{th} K^{-1} mol^{-1}	C_p(max.) / cal_{th} K^{-1} mol^{-1} l	h	Ref.
Fe_3O_4	113.3	118.88	164	66	98	1.4	33.2	117	6
Hyd-Fe_3O_4 [b]	117.0	123.0	139	68	71	1.18	27.2	(46.8)	1
Xtal-Fe_3O_4 [c]	117.30	(119)	140	140		1.2	109.6	28.8	1
Millar-Fe_3O_4	114.2		108	108		1.0	40		11
Zn(0.005)	110.57	119.09	142	126	16	1.1	53.7	36.1	1
Zn(0.010)	107.15		122	122		1.14	140		
Zn(0.066)	80		70	70		0.87	10.4		1
Cd(0.002-I) [d]	102.02	106.21	139	≈70	≈70	1.18	35	37	
Cd(0.002-II) [e]	121.25		148	148		1.29	73		
Cd(0.005)	114.66		155	155		1.3	101		1
Cd(0.010)	105.7		104	104		0.98	31		1

[a] ΔH_t's are enthalpy increments, ΔS_t's are entropy increments, and C_p's are heat capacities; subscripts on thermodynamic quantities: t, l, and h: total, lower-temperature, and higher-temperature transitions.

[b] Corresponds to Mn(0.008).

[c] Two large magnetic crystals.

[d] Annealing temperature 1370 K.

[e] Annealing temperature 1623 K.

TABLE 6. Thermodynamic properties at selected temperatures (cal_{th} = 4.184 J)

Sample Designation	T/K: 50	100	200	300	298.15
	Heat capacity, C_p/cal_{th} K^{-1} mol^{-1}				
Cd(0.002-I)	3.648	–	28.06	36.44	36.32
Zn(0.010)	3.856	13.579	28.01	23.48	36.34
Cd(0.002-II)	3.649	13.526	27.97	36.46	36.34
Fe_3O_4 [a]	3.558	13.063	27.87	36.16	36.04
	Entropy, $\{S°(T) - S°(0)\}$/cal_{th} K^{-1} mol^{-1}				
Cd(0.002-I)	1.366	–	22.08	35.17	34.94
Zn(0.010)	1.396	6.912	22.37	34.51	35.45
Cd(0.002-II)	1.340	6.805	22.32	35.40	35.17
Fe_3O_4 [a]	1.326	6.561	22.14	35.14	34.93
	Enthalpy, $\{H°(T) - H°(0)\}$/cal_{th} mol^{-1}				
Cd(0.002-I)	50.8	–	2722	5979	5912
Zn(0.010)	52.3	473.4	2751	6005	5938
Cd(0.002-II)	49.9	472.3	2763	6017	5949
Fe_3O_4 [a]	49.4	454.2	2750	5985	5955

[a] Reference 6.

ratio interval over which the defurcation occurs can be further narrowed to being between 0.005 and 0.010 per Fe_3O_4. Indeed, for a zinc mole ratio of 0.010, the lambda anomaly is not simple, exhibiting several shoulders and considerable broadening which we conclude to be incipient or vestigial furcation. A zinc dopant mole ratio of 0.01 per Fe_3O_4 is therefore, quite close to the critical mole ratio for the transformation from a furcated to an unfurcated lambda anomaly.

For cadmium, the critical mole ratio for the furcation of the heat-capacity anomaly is between 0.002 and 0.005 per Fe_3O_4. The furcation is quite pronounced in the Cd(0.002) sample and the critical mole ratio might, therefore, be somewhat larger than this. Thus a mole ratio 0.002 of Cd per Fe_3O_4 has an influence on the furcation of the phase transition that is equivalent to that of a mole ratio of Zn of 0.010 per Fe_3O_4. Thus, cadmium seems to be roughly five times as effective as zinc in causing the defurcation of the lambda anomaly associated with the Verwey transition.

The relative mole ratios at which Cd and Zn have equivalent effects on the phase transition provide some clue concerning the cogent crystal physical parameter. The crystal chemistries of zinc and cadmium in spinel oxides are quite similar, except for the larger unit-cell volume associated with cadmium substitution. It is instructive to consider whether relative unit-cell volumes and, therefore, electron concentrations are consistent with the dopant levels at which zinc and cadmium have equivalent effects on the Verwey transition. For Fe_3O_4, $ZnFe_2O_4$, and $CdFe_2O_4$, the 300 K cubic lattice constants are 0.8396 nm, 0.8445 nm, and 0.869 nm, respectively. Assuming Vegard's law is obeyed for cadmium- and zinc-doped Fe_3O_4, at least for the low dopant levels considered here (compare reference 4), then the lattice-constant increment produced by the dopant is 0.0049 nm mol^{-1} for Zn^{2+} and 0.0294 nm mol^{-1} for Cd^{2+}. Thus, the fact that Cd^{2+} is about 5 times as effective as Zn^{2+} in the obliteration of the furcation tends to correlate with the effect of the dopant on the linear dimensions of the lattice and not with the volume. If the relative influence of Zn^{2+} and Cd^{2+} on the character of the lambda anomaly were to arise from the relative change in the concentration of itinerant electrons, the furcation of the heat-capacity anomaly would not be expected to vanish until the mole ratio of Cd was 0.008 per Fe_3O_4, *i.e.* roughly four times the observed value.

The change in the lambda anomaly for sample Cd(0.002-II) upon annealing in CO_2 at 1623 K is remarkable. It is to be noted that this sample lost Cd at the higher annealing temperature and is, therefore, a pure Fe+O phase. The sample is expected to be slightly oxidized, however, to give a $n(Fe^{2+}+Fe^{3+})/n(Fe^{2+})$ ratio of 3.01. This corresponds to a mole ratio of vacancies of 1×10^{-3} per Fe_3O_4 which is much less than the mole ratio of vacancies in other oxidized magnetites on which measurements of physical properties have been made.[11] Indeed, the vacancy content of this sample is similar to that of Cd and Zn contents of the doped magnetites.

In relation to these dopants, the effects of vacancies are, therefore, rather large; and it is quite clear that vacancies cannot be regarded as innocuous. They must influence the Verwey transition not only through changes in the conduction-electron concentration but also more directly via their effects on electron-phonon interactions. A recent publication [12] also refers to a loss of the furcation of the lambda anomaly upon annealing a single crystal sample of Fe_3O_4 in apparent agreement

with our observation. In this study,[12] it was concluded that the annealing had a direct influence on the transition through the removal of residual stresses. The loss of the anomaly for the single crystal Fe_3O_4 could also arise, however, from changes in the sample stoichiometry as has been concluded in our investigation. The strain in our polycrystalline samples is expected to be much less than that in a single crystal grown according to Smilten's[12] technique and the loss of the furcation in Cd(0.002-II) sample cannot be due simply to the removal of strain. The substantially lower transition temperature of the Cd(0.002-II) is also at odds with an explanation of the loss of the furcation based on the presence of residual strain since in this case the transition temperature would be expected to increase upon annealing. It is also noteworthy that the enthalpies of transition of the single-crystal specimens showing evidence of residual stress were less than those for the samples reported on here.

It has been assumed that the effect of the stress is incidental to the thermal characteristics of the lambda anomaly at the Verwey transition. It is entirely possible, however, that the influence of an external stress on the phase transition may be similar to that occasioned by the changes in lattice constants resulting from the A-site dopants.

The authors appreciate the continuing support of the National Science Foundation and are grateful to Kungliga Fysiografiska Sällskapet for provision of a travel grant for Bengt Falk.

REFERENCES

1. Bartel, J. J.; Westrum, E. F., Jr. *J. Chem. Thermodynamics* **1975,** 7, 706; **1976,** 8, 575; **1976,** 8, 583.
2. Miyahara, Y. J. *J. Phys. Soc. Jpn* **1972,** 32, 629.
3. Evans, B. J.; Westrum, E. F., Jr. *Phys. Rev. B* **1972,** 5, 3791.
4. Bartel, J. J.; Westrum, E. F., Jr. *A.I.P. Conf. Proc.* **1973,** 10, 1393; **1975,** 24, 86.
5. Evans, B. J. *A.I.P. Conf. Proc.* **1975,** 24, 73.
6. Westrum, E. F., Jr.,; Grønvold, F. *J. Chem. Thermodynamics* **1969,** 1, 543.
7. Carlson, H. G. Ph.D. Thesis, The University of Michigan, Ann Arbor, Michigan, **1964;** Diss. Abstracts **1965,** 26, 1, 111.
8. Stimson, H. F. *J. Res. Nat. Bur. Stand. U.S.* **1961,** 42, 209.
9. Darken, L. S.; Gurry, R. W. *J. Am. Chem. Soc.* **1946,** 68, 798.
10. Evans, B. J.; Hafner, S. S. *J. Appl. Phys.* **1969,** 40, 1411.
11. Millar, R. W. *J. Am. Chem. Soc.* **1929,** 15, 215.
12. Annersten, H.; Hafner, S.S. *Z. Krist.* **1973,** 137, 321.
13. Matsui, M.; Todo, S.; Chikazumi, S. *J. Phys. Soc. Jpn* **1977,** 42, 1517.